The 6th IASPEI / IAEE International Symposium: Effects of Surface Geology on Seismic Motion
August 2021

ESG6 BLIND PREDICTION. 1D MODELING FOR STEPS 2 AND 3 BY INGV AND ENEA TEAM

Salomon Hailemikael[1], Giuseppe Di Giulio[2], Bordoni Paola[2], Maurizio Vassallo[2] and Giuliano Milana[2]

1 Researcher, ENEA Centro Ricerche Frascati, Rome, Italy (salomon.hailemikael@enea.it)
2 Researcher, INGV Istituto Nazionale Geofisica e Vulcanologia, Rome, Italy (giuseppe.digiulio@ingv.it; paola.bordoni@ingv.it; maurizio.vassallo@ingv.it; giuliano.milana@ingv.it)

ABSTRACT

This paper describes the analyses performed in the framework of ESG blind prediction steps 2 and 3, devoted to the simulation of the weak- (step 2) and strong-ground motions (step 3) recorded at the prediction site located on the Kumamoto plain (Japan) during the seismic sequence of 2016. We employed 1D equivalent-linear (EQL) simulations for predictions of step 2 and both EQL and nonlinear (NL) simulations in step 3. Models were built considering the results of step 1 in terms of shear-wave velocity profile and the available information on the site at regional and local scale distributed by the ESG committee. Nonlinear soil behavior was considered based on available laboratory tests on undisturbed soil samples and on the literature. Models were forced at the bedrock level by the signals recorded at the SEVO reference site assuming an outcropping motion boundary condition (elastic half space). The results showed significant horizontal ground motion amplification at the prediction site for both weak- and strong-motion input. The EQL results are characterized by substantial differences obtained using the NS and EW components of the input motions. The comparison between strong ground motion predictions using the EQL and NL approaches suggests a strong influence of nonlinear soil behavior for the shallow soil of the Kumamoto plain during the stronger earthquakes of the sequence.

Keywords: blind test step 2 and step 3, 1D simulation

INTRODUCTION

Steps 2 and 3 of the ESG 2021 blind prediction exercise are devoted to the simulation of both weak motions and strong motions recorded at the prediction site in the Kumamoto prefecture (KUMA) during the Kumamoto earthquake sequence. Simulated motions by each participant will be compared to the unpublished recordings obtained at KUMA for the Mj 5.9 earthquake occurred on April 16th 2016 (step 2), and for the Mj 6.4 foreshock (step 3) and Mj 7.3 mainshock (step 3) occurred on April 14th and 16th 2016. A simple assumption for performing such simulations is the 1D approximation by which the subsurface structure is represented as a stack of homogeneous isotropic horizontal viscoelastic layers overlying an elastic half-space subjected to horizontally polarized shear-waves (SH) with vertical incidence. Recently, a reappraisal about the capability of relatively simple 1D numerical simulations to reproduce observed ground motions has been the target of numerous papers (Thompson et al. 2012; Kaklamanos et al. 2013, Tao and Rathje 2020, among many others). Generally, it is found that the 1D approximation is not always sufficient to ensure that simulated ground motions adequately reproduce observations due to the complex (2D and 3D) subsurface conditions. In addition to such limitation, it is also well known that the commonly adopted equivalent-linear approach fails in reproducing observations once the maximum shear strain induced by the earthquake excitation in the soil exceeds some threshold level, estimated to be in the range 0.2-0.3% (Kim et al 2013; Yee et al 2013). Therefore, nonlinear ground simulations are recommended in case of strong ground motions (Stewart et al 2014). In this work, we present the results of 1D total stress simulations for the Mj 5.9 and Mj 6.4 horizontal ground motions whereas the M 7.3 mainshock was not modeled. In particular, the equivalent-linear method was employed for simulating the horizontal weak motions (Mj 5.9, step 2) and both the equivalent-linear (EQL) and nonlinear (NL) methods were used to simulate the horizontal strong-ground motions (Mj 6.4, step 3). For this last case, the results from the two approaches were compared to evaluate similarities and differences.

DESCRIPTION OF AVAILABLE DATA

Steps 2 and 3 of the ESG 2021 blind prediction exercise are devoted to the simulation of both weak motions and strong motions recorded at the prediction site in the Kumamoto prefecture (KUMA) during the Kumamoto earthquake sequence. Simulated motions by each participant will be compared to the unpublished recordings obtained at KUMA for the Mj 5.9 earthquake occurred on April 16th 2016 (step 2), and for the Mj 6.4 foreshock (step 3) and Mj 7.3 mainshock (step 3) occurred on April 14th and 16th 2016. A simple assumption for performing such simulations is the 1D approximation by which the subsurface structure is represented as a stack of homogeneous isotropic horizontal viscoelastic layers overlying an elastic half-space subjected to horizontally polarized shear-waves (SH) with vertical incidence. Recently, a reappraisal about the capability of relatively simple 1D numerical simulations to reproduce observed ground motions has been the target of numerous papers (Thompson et al. 2012; Kaklamanos et al. 2013, Tao and Rathje 2020, among many others). Generally, it is found that the 1D approximation is not always sufficient to ensure that simulated ground motions adequately reproduce observations due to the complex (2D and 3D) subsurface conditions. In addition to such limitation, it is also well known that the commonly adopted equivalent-linear approach fails in reproducing observations once the maximum shear strain induced by the earthquake excitation in the soil exceeds some threshold level, estimated to be in the range 0.2-0.3% (Kim et al 2013; Yee et al 2013). Therefore, nonlinear ground simulations are recommended in case of strong ground motions (Stewart et al 2014). In this work, we present the results of 1D total stress simulations for the Mj 5.9 and Mj 6.4 horizontal ground motions whereas the M 7.3 mainshock was not modeled. In particular, the equivalent-linear method was employed for simulating the horizontal weak motions (Mj 5.9, step 2) and both the equivalent-linear (EQL) and nonlinear (NL) methods were used to simulate the horizontal strong-ground motions (Mj 6.4, step 3). For this last case, the results from the two approaches were compared to evaluate similarities and differences.

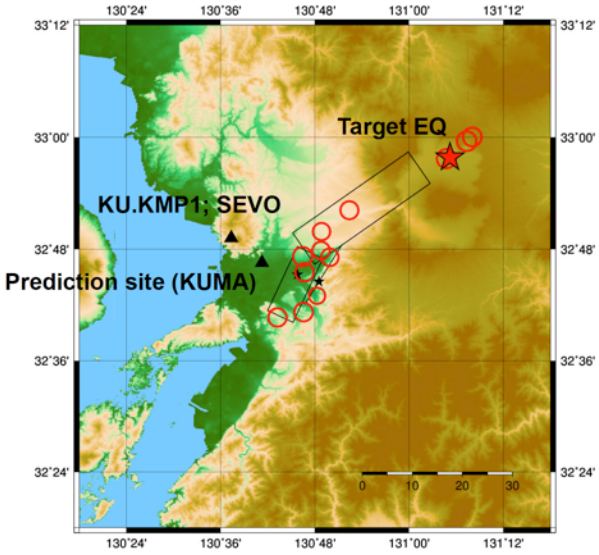

Figure 1. Map showing the location of the prediction KUMA and reference SEVO sites. The distribution of earthquakes belonging to the Kumamoto sequence for which recordings at the sites are available are also shown as red circles. The unpublished recordings of the blind prediction exercise step 2 refer to the aftershock (red star) of the sequence.

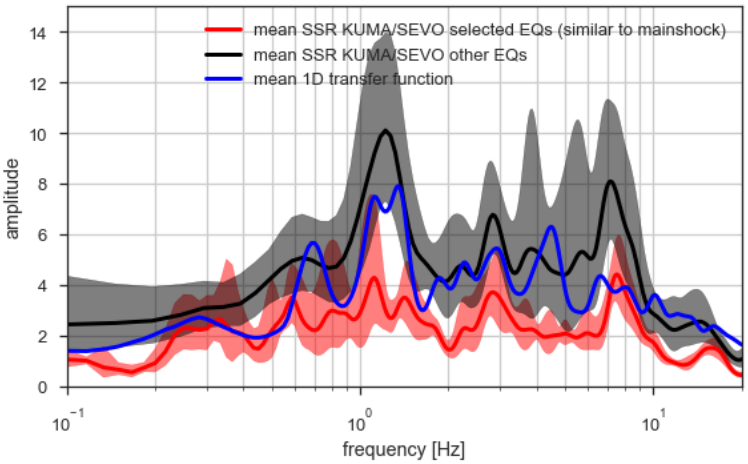

Figure 2. Average SSR calculated between KUMA and SEVO recordings. Functions are calculated for earthquakes closer to the Mj 5.9 earthquake (solid red curve) and for earthquakes farther from it and closer to the Kumamoto plain (solid black curve). The shaded area represents the average ± 1 standard deviation. The theoretical 1D transfer function of the EQL model obtained for step 2 of the blind prediction is also shown (solid blue curve, see text for more details).

METHODS

We simulated the weak motions (Mj 5.9, step 2) observed at the prediction site KUMA by the STRATA code, which allows performing 1D total stress site ground response analysis in the frequency domain (Kottke and Rathje, 2008). This code takes into account nonlinearity of subsurface materials through the equivalent-linear (EQL) approach (Schnabel et al., 1972), an iterative procedure for which the assigned properties of the viscoelastic sub-surface layers, namely normalized shear modulus (G/G0) and material damping ratio (D), are iteratively adjusted to be consistent with the effective level of shear strain (γ %) induced by the input motion. The effective strain ratio was fixed to 0.55 and maximum iteration number was set equal to 20. EQL implementation needs that each visco-elastic model layer is characterized by values of thickness, density, shear-wave velocity (Vs) and modulus reduction (G/G0) and damping (D) curves as a function of (Table 1). In principle, STRATA software allows taking into account variation of thickness, velocity and nonlinear properties of the model but we decided to proceed in the simulation without including variations.
In addition to EQL 1D simulations, we also performed a 1D total stress site ground response analysis by the Deepsoil software (Hashash et al., 2020) to predict horizontal strong ground motions (Mj 6.4, step 3). This finite-difference code allows performing fully nonlinear (NL) site response analysis in the time-domain by integrating the equation of motion in small time steps. This approach fully accounts for nonlinear behavior of subsurface materials through cyclic nonlinear stress-strain models.
As a constitutive model, we used an extended version of the MKZ model developed by Matasović and Vucetic (1993) for the shallower layers (Table 2). The MRDF pressure-dependent hyperbolic model procedure (Hashash et al 2020) was used to fit nonlinear modulus reduction (G/Gmax vs shear strain) and damping (D vs shear strain) curves associated with each model layer. This procedure includes a frequency-independent damping as proposed by Phillips and Hashash (2009).
Input motions were the horizontal ground motions (NS and EW components) recordings acquired at SEVO for the Mj 5.9 (step 2) and Mj 6.4 earthquakes (step 3). These signals were baseline corrected (processed by de-trending, zero padding and high-pass filtering with 0.1 Hz corner frequency) and applied at the half-space level as acceleration time-history in units of g by implementing an elastic base boundary condition at the half-space, therefore considering the input as outcropping motions for both EQL and NL 1D simulations.

1D EQL AND NL MODELS DESCRIPTION

To define the sub-surface model, as participants of the ESG blind prediction, we decided to rely on the Vs model evaluated in step 1 by our team through inversion of seismic passive data (Di Giulio et al. 2021). Model parameters for the EQL prediction are summarized in Table 1. For the shallower layers, nonlinear modulus reduction and damping curves were drawn from the laboratory tests and from the literature (Rollins et al 1998), taking into account the borehole information included in the ESG report (Kumamoto Eq. Ground Structure Survey). For the deeper layers, we assumed linear visco-elastic stress-strain behavior with constant damping ratio of 1 %. This value was selected by considering the fit between the theoretical transfer function (calculated for the step 2 of the blind prediction exercise, Fig. 2 blue curve) and the empirical transfer function calculated between KUMA and SEVO recordings (black and red curves in Fig. 2) provided by the ESG committee. The fit was evaluated also in terms of time series and Fourier Amplitude Spectra (Fig. 3). Density model was built considering the results of laboratory testing provided by the ESG committee and the information of the JIVSM (Japan Integrated Velocity Structure Model, Koketsu et al. 2014) and the Chimoto et al. (2016) model. For the nonlinear model of step 3, the Vs subsurface model that we evaluated in step 1 was adapted to the layer discretization needed to correctly perform the nonlinear analysis, namely by fulfilling the following condition: sub-layer thickness h <= Vs/(4 *f_{max}), where f_{max} is the maximum frequency of analysis and was set equal to 30 Hz. The 1D nonlinear model is summarized in table 2, including layer discretization (n# of sub-layers and thickness of each sub-layer). Model was built similarly to what was described for the EQL case. Table 2 also includes target modulus reduction and damping curves for the fitting of the MRDF pressure-dependent hyperbolic model. Similarly to the EQL case, we assumed linear visco-elastic stress-strain behavior with constant damping ratio of 1 % for the deeper layers (i.e. at depth larger about 80 m).

Table 1. 1D EQL model parameters

Layer number	Depth (m)	Thickness (m)	Density (KN/m^3)	Vs (m/s)	Modulus reduction and damping curves
1	0.00	2.79	14	143.00	T1 sample
2	2.79	2.79	14	166.00	T1 sample
3	5.58	2.79	13	189.00	T2 sample
4	8.37	2.79	13	213.00	T2 sample
5	11.16	2.79	19	236.00	T3 sample
6	13.95	17.00	18	253.00	T4 sample
7	30.95	6.91	18	253.00	T4 sample
8	37.86	12.87	18	406.00	Rollins et al. 1998
9	50.73	29.29	18	420.00	Rollins et al. 1998
10	80.02	80.81	21	949.00	Linear
11	160.83	231.25	21	1020.00	Linear
12	392.08	1092.94	23	1700.00	Linear
13-Half space	1485.02	#	27	3728.00	#

Table 2. 1D NL model parameters

Layer	n# of sub-layers	sub-layer thickness (m)	sub-layer density (KN/m^3)	Vs (m/s)	Constitutive model
1	3	1	14	143.00	MKZ
2	3	1	14	166.00	MKZ
3	3	1	13	189.00	MKZ
4	3	1	13	213.00	MKZ
5	3	1	19	236.00	MKZ
6	8	2	18	253.00	MKZ
7	3	2	18	253.00	MKZ
8	4	3	18	406.00	MKZ
9	9	3.5	18	420.00	MKZ
10	10	8	21	949.00	Linear
11	27	8.5	21	1020.00	Linear
12	77	14	23	1700.00	Linear
13-Half space	#	#	27	3728.00	#

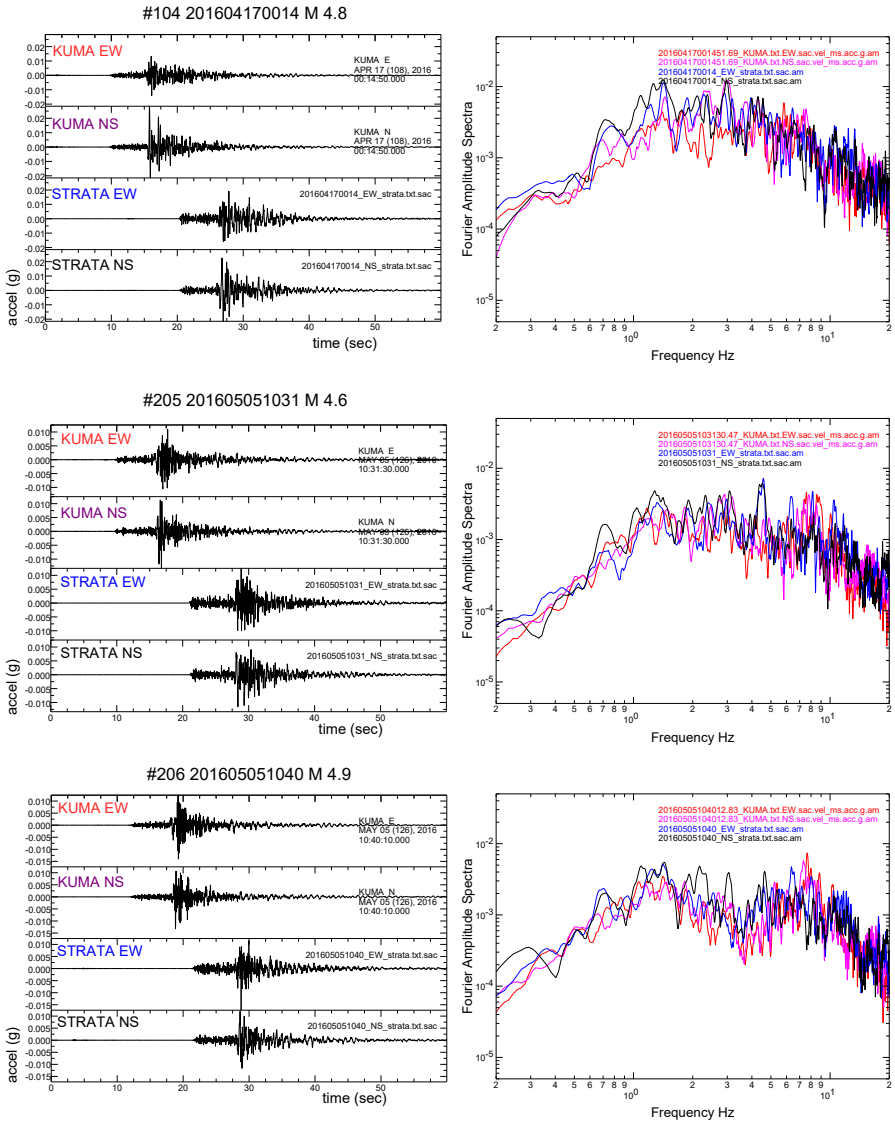

Figure 3. Comparison between recordings obtained at KUMA and 1D EQL (STRATA) predictions for the subset of earthquake signals (closer to the Mj 5.9 earthquake) distributed by the ESG committee in step 2. The comparison is shown in terms of horizontal ground acceleration at the surface (left panel) and in terms of Fourier amplitude spectra (right panel).

RESULTS

The 1D simulations showed significant horizontal ground motion amplification at the prediction site for both weak- and strong-motion input. The predicted time series of the M 5.9 earthquake obtained for step 2 using the EQL approach show PGA of about 0.35 g for the EW component and of about 0.05 g for the NS component (Fig. 4 top panel). In terms of output elastic response spectra, the maximum values of spectral ordinates (PSA) are reached in the interval 0.5-0.8 s on the NS component, which shows values larger than 0.125 g, whereas maxima of the spectral ordinates are shown for periods lower than 0.5 s on the EW component (PSA of about 0.085 g). In those intervals showing the maximum spectral ordinates, the output is 5 times larger than the input for the NS and about 3.5 times larger for the EW component (Fig. 4 bottom right panel). The maximum shear strain (equal to 0.015%) is reached for the NS component at a depth of about 37 m.

The output obtained for step 3 allows us the comparison between horizontal strong ground motion predictions (Mj 6.4) obtained using the EQL and NL approaches. The output PGA for the EQL

simulations is about 0.33 g for both horizontal components, whereas the PGA is about 0.18 g for the EW component and 0.16 g for the NS component in the case of the NL predictions (Fig 5, top and middle-upper panels). In terms of PSA values EQL results show maxima larger than 0.7 g in the period interval 0.8-1.1 seconds and secondary peaks with amplitude of about 0.6 g for periods lower than 0.5 s (Fig 5, bottom right panel). The NL simulations predicted several peaks in the elastic response spectra for the EW and NS components with similar amplitude around 0.4 g in the period range T< 1.2 s (Fig 5, bottom right panel). This means that the EQL predictions in terms of maximum PSA are 75% larger than the NL ones. In terms of maximum shear strain, the peak strain is reached at the same depth as in step 2 for both components and approaches. The differences in terms of strain profile between the two approaches are shown in Fig. 6; for the EW component, the peak shear-strain calculated with EQL approach (about 0.2%) is about double that of the NL one (Fig 6 left panel). For the NS component the differences are lower, the peak strain is about 0.16% for the NL case whereas it is 0.22 % for the EQL case.
These results suggest that a significant nonlinear behavior has been induced by the strong ground motions (Mj 6.4) for the Kumamoto Plain shallow soils.

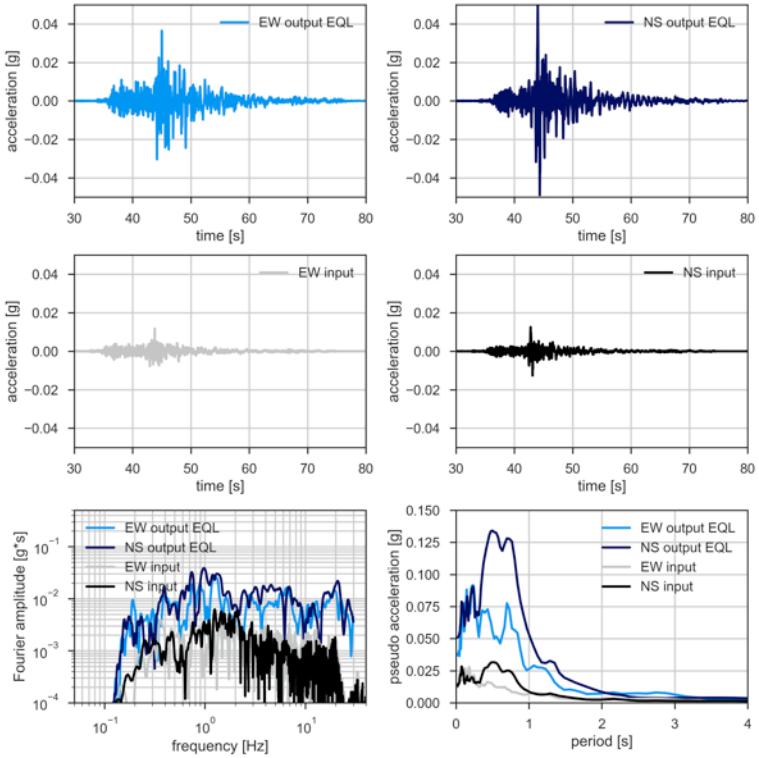

Figure 4. 1D EQL modeling predictions for the ESG step 2. Output acceleration time-histories for the EW and NS components (top panel) along with input motions recorded at SEVO (middle panel). Fourier amplitude spectra and elastic response spectra of each signal are also shown (bottom panel).

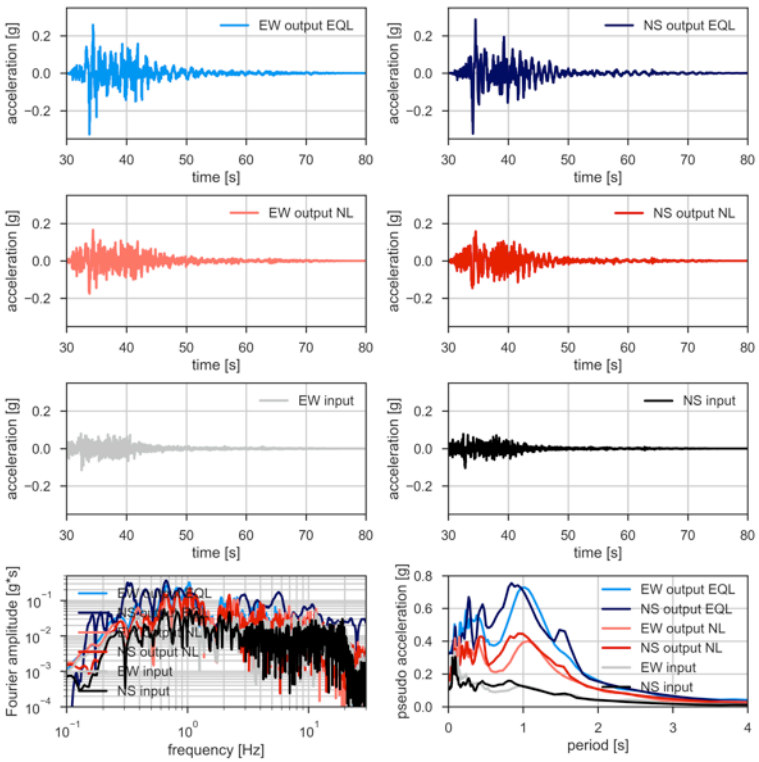

Figure 5. 1D EQL and NL modeling predictions for the ESG step 3. Output EQL acceleration time-histories for the EW and NS components (top panel), the same predictions are calculated for the NL approach (middle-upper panel) along with input motions recorded at SEVO (middle-lower panel). Fourier amplitude spectra and elastic response spectra of each signal are also shown (bottom panel).

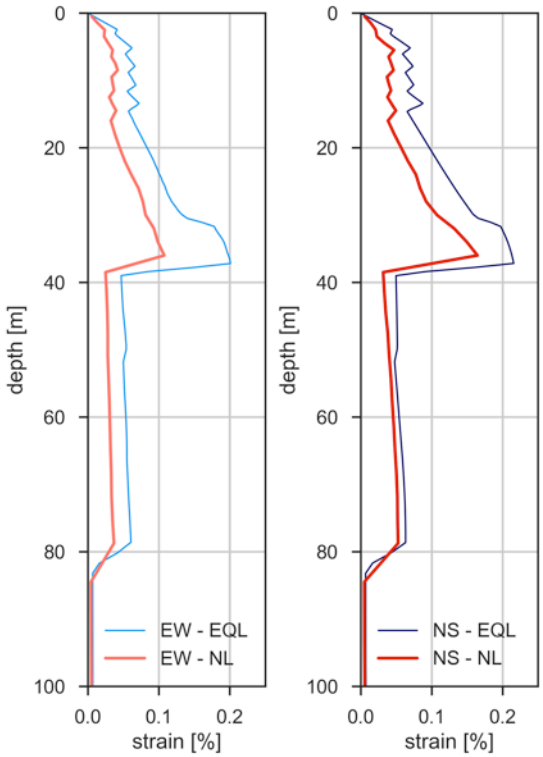

Figure 6. 1D EQL and NL shear strain profile predictions for the ESG step 3 considering the EW component (left panel) and NS component (right panel) of the input motions.

REFERENCES

Borcherdt, R. D. (1994). "Estimates of site-dependent response spectra for design (methodology and justification)", *Earthquake Spectra*, **10** ,617 –653.

Bordoni P., Milana G., Lucarelli A., Di Giulio G., Hailemikael S., Vassallo M. (2021). "Prediction of Kumamoto foreshocks strong motion from linear and nonlinear 2D modeling", ESG6 Blind Prediction Step3

Chimoto et al. (2016). "Estimation of shallow S-wave velocity structure using microtremor array exploration at temporary strong motion observation stations for aftershocks of the 2016 Kumamoto earthquake", *Earth, Planets and Space*, **68**(206), https://doi.org/10.1186/s40623-016-0581-3

Di Giulio, G., et al. (2021). "ESG6 Blind Prediction, Step1 by INGV and ENEA team".

Hashash, Y.M.A., Musgrove, M.I., Harmon, J.A., Ilhan, O., Xing, G., Numanoglu, O., Groholski, D.R., Phillips, C.A., and Park, D., (2020). "DEEPSOIL 7.0, User Manual". Urbana, IL, Board of Trustees of University of Illinois at Urbana-Champaign.

Kaklamanos J., B.A. Bradley, E.M. Thompson & L.G. Baise (2013). "Critical parameters affecting bias and variability in site-response analyses using KiK-net downhole array data". *Bulletin of the Seismological Society of America,* **103**(3), 1733-1749.

Kim B, Hashash YMA (2013). "Site response analysis using downhole array recordings during the March 2011 Tohoku-Oki earthquake and the effect of long-duration ground motions". *Earthq Spectra*, **29**:S37–54.

Koketsu, K., H. Miyake, H. Suzuki (2012). "Japan Integrated Velocity Structure Model Version 1", *Proceedings of the 15th World Conference on Earthquake Engineering*, Lisbon, Portugal, Oct. 12–17, Paper No. 1773.

Kottke, A. R., and E. M. Rathje, (2008). "Technical manual for Strata". Report No.: 2008/10. Pacific Earthquake Engineering Research Center, University of California, Berkeley.

Phillips C, Hashash YMA, (2009). "Damping formulation for nonlinear 1D site response analyses". *Soil Dyn Earthq Eng*, **29**:1143–58.

Matasović N, Vucetic M, (1993). "Cyclic characterization of liquefiable sands". *J Geotech Eng*, **119**:1805 22.